Evaluation of greening and highly reflective materials from three perspectives

Saori Yumino[1], Taiki Uchida[1], Akashi Mochida[1], Hikaru Kobayashi[1], Kiyoshi Sasaki[2]
[1] *Tohoku University, #1206 6-6-11 Aoba Aramaki-Aza Aoba-ku Sendai, Japan, yumino@sabine.pln.archi.tohoku.ac.jp, taiki@sabine.pln.archi.tohoku.ac.jp, mochida@sabine.pln.archi.tohoku.ac.jp, kobayashi@sabine.pln.archi.tohoku.ac.jp*
2 Institute of Technology, SHIMIZU CORPORATION, 3-4-17 Ecchujima Koto-ku Tokyo, Japan, k_sasaki@shimz.co.jp

dated: 15 May 2015

1. Introduction

Urban areas are subject to increased temperatures due to the influence of global warming and urbanization, and various techniques have been studied as countermeasures. Most studies that compared the effects of several countermeasure techniques assumed a single perspective: either that of energy savings, suppression of effluent sensible heat, or improvement of the thermal environment in pedestrian spaces. However, these aims often conflict with one another. Therefore, great difficulties still remain when policymakers and urban planners attempt to select proper countermeasure techniques, despite the enormous accumulation of knowledge. To overcome the difficulties associated with the selection of proper countermeasures against urban warming, the purposes of such countermeasures should be considered. First, there are two aspects to these countermeasures: mitigation and adaptation. Mitigation refers to the removal of the causes of the phenomenon, whereas adaptation refers to a reduction in the effects of the phenomenon, even if the magnitude of the phenomenon does not change. Second, ongoing urban warming is being caused by both global warming and the creation of urban heat islands (UHIs). Global warming is caused by the rising concentration of greenhouse gases, which affects temperatures worldwide, whereas a UHI is caused by a modification in land-use from a natural environment into a built environment with the intensive energy consumption in such urban areas resulting in anthropogenic heat release. Thus, the energy savings resulting in CO_2 emission reductions are essential for mitigating global warming, and the suppression of effluent sensible heat from urban surfaces is essential for mitigating UHIs. Different countermeasures are needed to mitigate these two phenomena, global warming and UHIs, and to adapt to urban warming. However, the distinctions between countermeasures used (1) to mitigate global warming, (2) to mitigate UHIs, and (3) to adapt to urban warming remain vague. To assess the effects of countermeasures used to mitigate global warming, mitigate UHIs, and adapt to urban warming simultaneously, a new assessment system was proposed in our previous study (Yumino et al., 2015). In the present paper, the results of two simulations are reported: one is the evaluation of the effects of greening and highly reflective material applied to vertical walls in a town-block model and another is the evaluation of the effects of roadside trees in an actual urban area.

2. Assessment system

The focus regions for assessing the effects of countermeasures against urban warming differed among researchers. Although the focus region is closely related to the purpose of countermeasures, the regions used in the assessment were determined without clearly recognizing the distinction between the countermeasures used to mitigate global warming, to mitigate UHIs, and to adapt to urban warming in many previous studies. This caused unnecessary misunderstanding and confusion in the discussions among the researchers about the assessment of the countermeasures for urban warming. To avoid such confusion, it is important to clearly recognize the purposes of the countermeasures and consider the appropriate domains for assessment according to their purposes. In this study, three domains for evaluating the effects of countermeasures for mitigating global warming, mitigating UHIs, and adapting to urban warming are set in an assessment system. Different assessment indices corresponding to each domain (Fig. 1) are proposed. First, in order to assess the mitigation of global warming, Domain A, which represents building interiors, is defined, and the energy consumption of heating, ventilation, and air conditioning (HVAC) systems is calculated. Next, to assess the mitigation of UHIs, Domain B, which represents the urban atmosphere, is defined, and the amount of effluent heat from the urban surface to outdoor air is evaluated. The pedestrian space within Domain B is defined as another domain, Domain C, used to assess the adaptation to urban warming. The standard effective temperature (SET*) and wet bulb globe temperature (WBGT) are calculated in this domain. Details of the formulation of the assessment indices for each domain, and the proceres for calculating the assessment indices were described in Yumino et al., (2015).

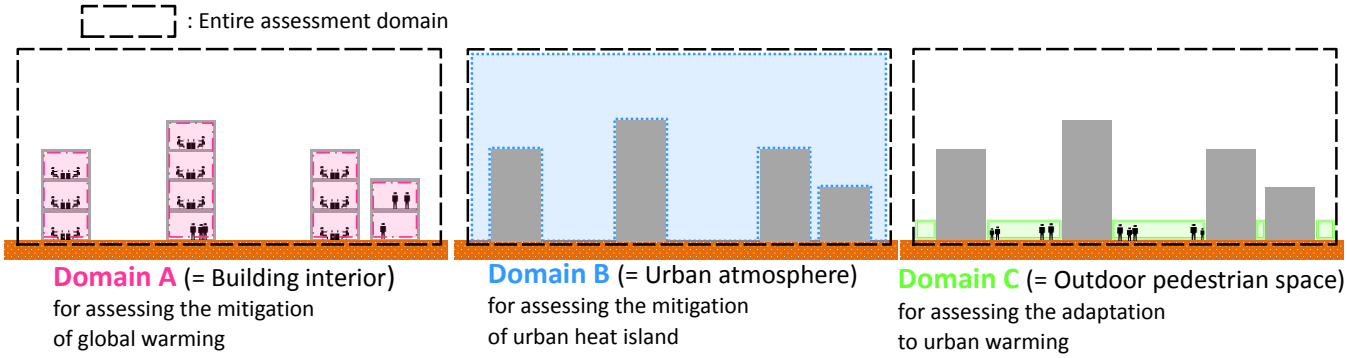

Fig.1 Concept of the assessment system

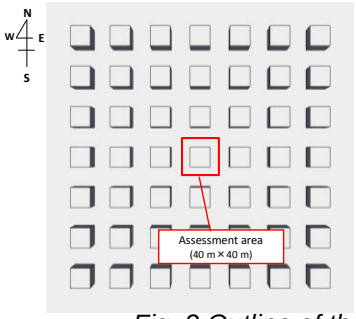

Town block model

Building coverage ratio[%]:	25
Building width and height, road width[m]:	20
Building use:	Business Office
Location:	Otemachi, Tokyo

Roofs

Albedo[-]:	0.2
Emissivity[-]:	0.1
Surface wetness[-]:	0.0

Road

Albedo[-]:	0.2
Emissivity[-]:	1.0
Surface wetness[-]:	0.0

Fig. 2 Outline of the town block model

Table 1 Details of the office building

Building Structures	Number of stories [-]	5
	Floor height [m]	4
	Ceiling height [m]	2.8
	Rentable area ratio [-]	0.8
	Building volume available for work purposes [m^3]	4390
HVAC System	Ventilation rate [m^3/s]	2.18
	COP [-]	3
	Air temperature set point [° C]	28
	Running time [h]	(7-21)
Settings Related to Indoor Heat Balance	Interior heat generation	Given by the guidelines for calculating building energy consumption in Japan (NILIM and BRI, 2013)
	Heat capacity of materials inside the building, such as furniture and documents	

Table 2 Calculation cases

Case name	Material	Albedo [-]	Emissivity [-]	Surface wetness [-]	Window ratio [-]
Concrete	Concrete	0.2	1.0	0.0	0.0
Highref	Highly reflective material	0.6	1.0	0.0	0.0
Greening	Greening	0.2	1.0	0.3	0.0

3. Evaluation of the effect of greening and highly reflective materials applied to vertical walls

In this section, the assessment system described above was applied to the ideal town-block model. The thermal environments in three cases were considered: all vertical walls in the town block model were concrete, the vertical walls were of a highly reflective material, and greening was applied to the walls. These three situations were simulated to evaluate the effects of highly reflective material, and of greening, from the three stated perspectives of urban warming countermeasures.

3.1 Simulation outline

3.1.1 Simulation target

The settings for the town block model (Fig. 2 and Table 1) summarize the details of the office building utilized.

3.1.2 Calculation Cases

In this study, three situations were simulated and assessed using different physical properties of the vertical wall surfaces of the town block model: (1) concrete, (2) a highly reflective material, and (3) greening. The physical properties of each case are listed in Table 2. For all cases, the physical properties of the roof and road surfaces were identical, and the window ratio for each wall was set to zero. This was because the effects of differing physical properties of only vertical wall surfaces on the thermal environment were investigated as an initial step.

3.1.3 Calculation settings

To investigate change in the thermal environment due to changes in thermal property, simulations of radiation and conduction and non-isothermal CFD were conducted for each case. Calculation conditions are described in Yumino et al., (2015).

3.2 Simulation results

(1) Mean radiant temperature (MRT) (Fig. 3)

The horizontal distributions of MRT values at a height of 1.25 m at 14:00 are compared in Fig. 3. The MRT values around the highly reflective material surface were higher in the overall assessment area than those of concrete, because of the increase in reflected solar radiation to the pedestrian space. In contrast, the MRT values around the greening material were lower than those of concrete.

(2) Horizontal distributions of wind vector and air temperature (Fig. 4)

The entire pattern of flows and air temperatures was almost identical for the concrete and highly reflective surfaces, but that of the greening material differed. All air temperatures were lower where greening materials were used.

(3) SET* (Fig. 5)

The SET* values in the case of the highly reflective material was the highest because of the deteriorating radiant environment. The SET* values for the greening material case increased in the area near the west wall of the building because of the increase in the humidity, even though the radiant environment was much improved around the greening material.

(4) WBGT (Fig. 6)

The horizontal distributions of WBGT in each case showed a tendency similar to that of the SET*.

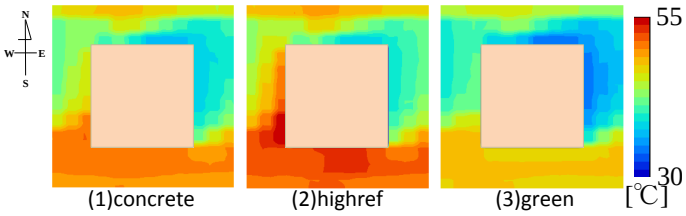

Fig. 3 Horizontal distributions of MRT (at 1.25 m height)

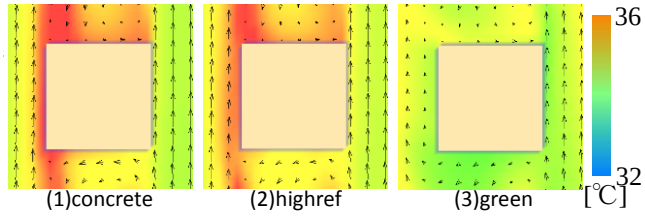

Fig. 4 Horizontal distributions of wind vector and air temperature (at 1.25 m height)

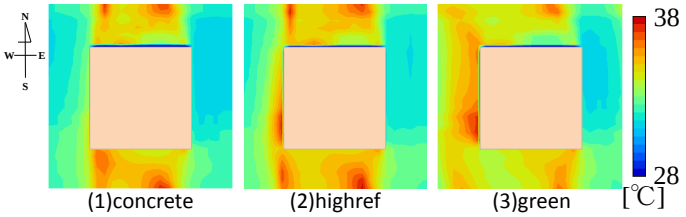

Fig. 5 Horizontal distributions of SET (at 1.25 m height)*

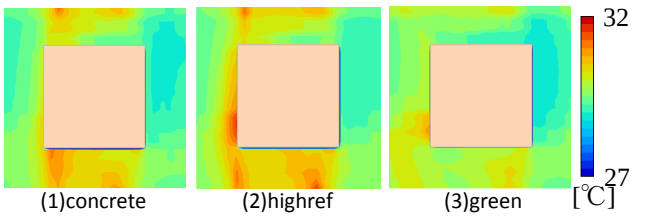

Fig. 6 Horizontal distributions of WBGT (at 1.25 m height)

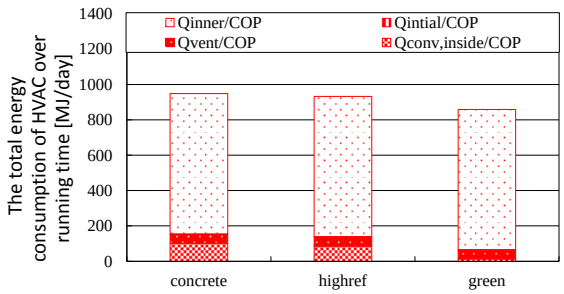

Fig. 7 Energy consumption of the HVAC system

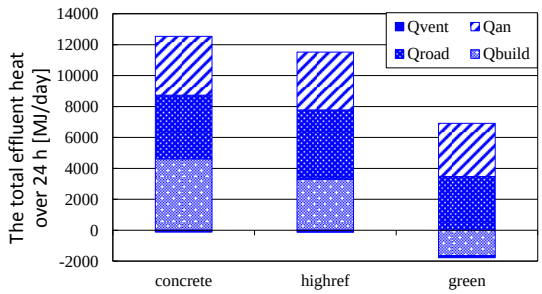

Fig. 8 Net effluent sensible heat from urban surfaces

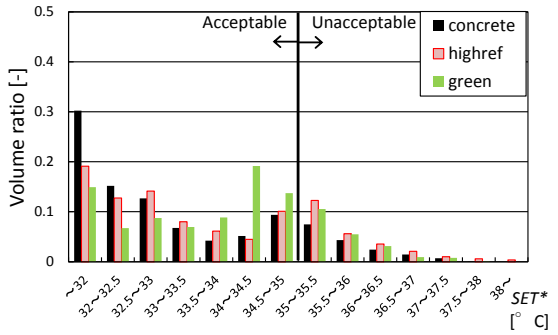

Fig. 9 Cumulative distributions of SET within the pedestrian space*

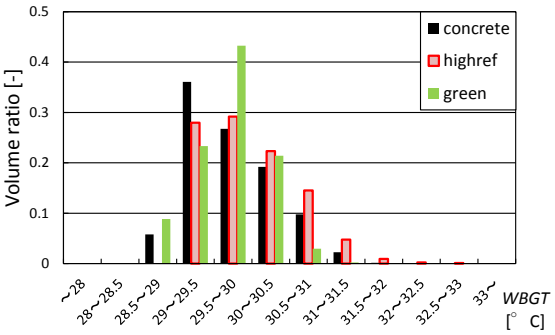

Fig. 10 Cumulative WBGT distributions within the pedestrian space

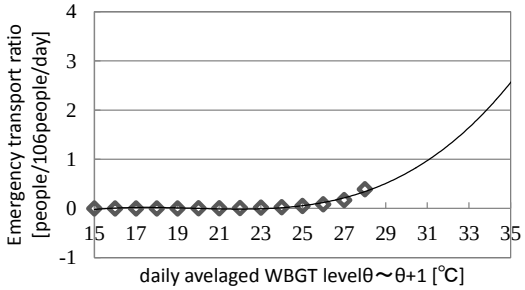

Fig. 11 Emergency transport probability curve for heatstroke in Tokyo

Table 3 Assessment result of the effect of highly reflective material and greening

Case	Energy consumption of HVAC [MJ] [Domain A]	Net effluent sensible heat from urban surfaces [MJ] [Domain B]	Acceptable volume ratio evaluated on the basis of SET* (<35°C) [Domain C]	Estimated emergency transport ratio of heatstroke [person/10^6 people/day] [Domain C]
Concrete	950	12400	84[%]	0.66
Highref	930	11400	75[%]	0.71
Greening	860	5100	79[%]	0.65

3.3 Assessment results

(1) Assessment of global warming mitigation

Fig. 7 compares the total energy consumption over the running time of the HVAC system. In the cases with greening and highly reflective materials, the energy consumption values were lower than those observed for the concrete surfaces. The energy consumption in the case with highly reflective material was lower by 2%, and that in the case with greening was lower by 9%, than for concrete surfaces. The differences in the energy consumption of the HVAC system among these three cases was mainly caused by differences in influent heat, due to convection from the surfaces of the interior building walls to the indoor air.

(2) Assessment of UHI mitigation

The amount of net effluent sensible heat from the urban surface in each case is shown in Fig. 8. In the case of the greening material, the amount of net effluent sensible heat decreased significantly because of the reduction in the effluent sensible heat convected from the wall surface.

(3) Assessment of the adaptation to urban warming

(a) Assessment in terms of thermal comfort

Fig. 9 shows the cumulative distributions of SET* within the pedestrian space, which ranged from ground level to a height of 2 m. In this study, the acceptable maximum limit of SET* was considered to be 35 °C. The vertical black line in Fig. 9 indicates a temperature of 35 °C. In the case of the highly reflective material, the volume where SET* exceeded 35 °C increased overall, and the acceptable volume ratio in the cases with highly reflective material and greening were 75% and 79%, whereas that of the concrete surface was 84%.

(b) Health hazard assessment

Fig. 10 shows the cumulative distributions of WBGT within the pedestrian space, which ranged from ground level to a height of 2 m. In the case with highly reflective material, the volumes with higher WBGT values increased as compared to the concrete surfaces, but the dispersion of WBGT in the greening case decreased as compared to the concrete surfaces.

Fig. 11 illustrates emergency transport probability curves for heatstroke in Tokyo. This curve is based on emergency transport data obtained from the Tokyo Fire Department. From this curve, and the spatial averages of WBGT within pedestrian spaces in each case, the values of the estimated emergency transport ratio, namely the risk of heatstroke, can be calculated. The risk values of the cases with concrete, highly reflective material, and greened surfaces were 0.66, 0.71, and 0.65 [person/10^6 people/day], respectively.

(4) Assessment results

Table 3 summarizes the assessment result in each domain. Greening and highly reflective materials have positive effects on the mitigation of global warming and for UHIs under the analysis conditions assumed here, whereas highly reflective materials have an adverse effect on the adaptation to urban warming.

4. Evaluation of the effect of roadside trees in an actual urban area

This chapter shows the process of evaluating the effects of roadside trees.

4.1 Simulation outline

4.1.1 Simulation target

An area around a wide intersection in Shinbashi, typical business district in Tokyo, Japan, was selected as the simulation target because the thermal environment around wide intersections is often considerably worse, according to a report by Ministry of the Environment in Japan (2013). In terms of reduction of calculation cost, several buildings located in the same town block were modeled as a lumped building. The computational domain is shown in Fig. 11. The calculation date selected was 20 July 2002. The weather condition on this day was regarded as a typical summer condition in the CASBEE-HI manual, (2010).

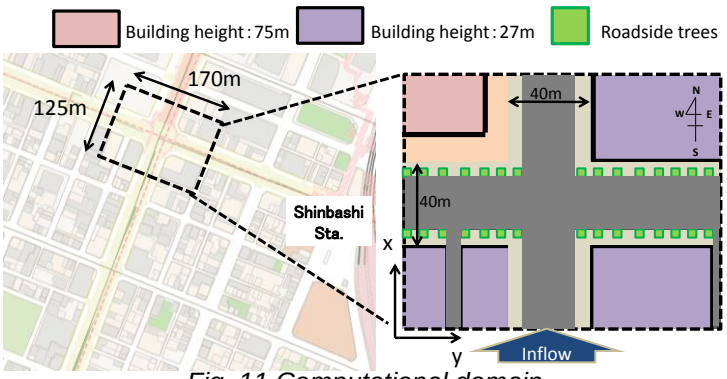

Fig. 11 Computational domain

Table 4 Settings of roadside trees

Tree crown height [m]	Tree height [m]	Tree crown width [m]	Pitch of tree planting [m]	Leaf area density [m^2/m^3]	Surface Wetness [-]
3	13.5	5	10	0.56	0.44

Table 5 Calculation conditions for the unsteady radiation and conduction simulation

Calculation date	July 20th 2002
Calculation period	For 48 h from 0:00 a.m. on July 19th
Meteorological data	Data provided by meteorological observatory
Mesh number (x × y × z)	34×15×13
Domain size (x[m] × y[m] × z[m])	170×125×275

Table 6 Calculation conditions for the CFD simulation

Calculation time	14:00
Mesh number (x × y × z)	69×57×52
Domain size (x[m] × y[m] × z[m])	172.5×875×550
Turbulence model	Durbin model (Durbin, 1996)
Discretization scheme of convective teams of transport equations	QUICK scheme

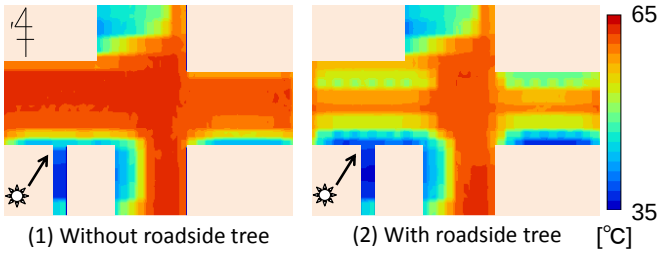

Fig. 12 Horizontal distributions of MRT (at 1.5 m height)

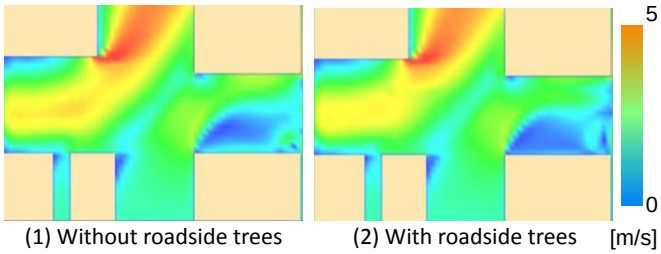

Fig. 13 Horizontal distributions of wind velocity (at 1.5 m height)

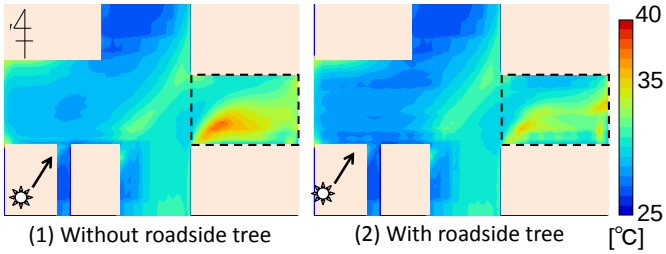

Fig. 14 Horizontal distributions of SET (at 1.5 m height)*

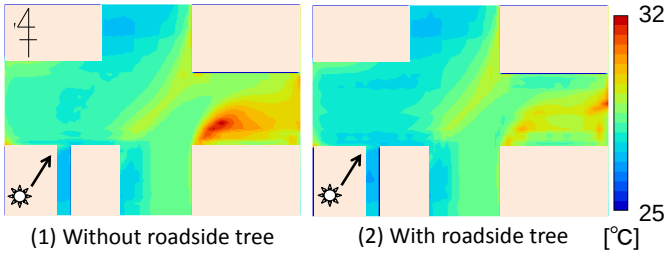

Fig. 15 Horizontal distributions of WBGT (at 1.5 m height)

4.1.2 Calculation cases

Two situations were simulated to investigate the effects of roadside trees from the three perspectives of urban warming countermeasure: with roadside trees and without roadside trees. The shape and pitch of the trees planted were determined by reference to a report by the Ministry of the Environment in Japan (2013). Leaf area density and surface wetness were set by the results of our measurements, on the assumption that roadside trees are in a controlled environment and that the amount of transpiration from roadside trees was large (Table 4). In the case with roadside trees, trees were planted along with road in the east-west direction (Fig. 11).

4.1.3 Calculation setup

Tables 5 and 6 show the calculation conditions of these simulations. The settings related to HVAC system and wall properties for assumed office buildings were almost the same as described in Section 3.1.1, but the window ratio was set to 0.5 in this calculation.

4.2 Simulation results

(1) MRT (Fig. 12)

The horizontal distributions of MRT at a height of 1.5 m are illustrated in Fig. 12. The difference in the MRT values due to the effect of the roadside trees was observed on the north side of the road in the east-west direction.

(2) Wind velocity (Fig. 13)

There was an area of high wind speed on the northwest side of the computational domain in both cases due to modification of the wind flow by a tall building.

(3) SET* (Fig. 14)

In the northwest part of the computational domain, SET* was low in both cases due to high wind speed, while the difference between SET* values in each case was caused by the difference between MRT values on the east side of the computational domain, where building heights were uniform and wind speed was relatively low.

(4) WBGT (Fig. 15)

The horizontal distributions of WBGT in each case showed a tendency similar to those of the SET*.

4.3 Assessment results

(1) Assessment of global warming mitigation

In Fig. 16, the total energy consumption is compared over the running time of the HVAC system. The energy consumption values in both cases were almost the same. However, the influent heat convected from the building interior wall surfaces to the indoor air, and the influent heat from a radiation-transmitting window, were slightly smaller with roadside trees, than without them.

(2) Assessment of UHI mitigation

The amount of net effluent sensible heat from the urban surface in each case is shown in Fig. 17. In the case with roadside trees, the amount of net effluent sensible heat decreased by 5% compared to the case without roadside trees. This was because of a reduction in the effluent sensible heat convected from the road surface when it was shaded by trees.

(3) Assessment of the adaptation to urban warming

(a) Assessment in terms of thermal comfort

Fig. 18 shows the cumulative distributions of SET* within the pedestrian space, which ranged from ground level to a height of 2 m. In the case with roadside trees, the area where SET* fell below the acceptable limit (35 °C) increased compare to the case without roadside trees. The acceptable volume ratios considering the entire pedestrian space in both cases were very high because the high-wind-speed area was large. The modification of wind flow by a tall building, and the resulting high wind speed strongly affected the reduction of SET* under the

conditions assumed in this calculation. However, focusing only on the east side of the computational domain, where the wind speed was relatively low, the acceptable volume ratios in the cases with and without roadside trees were 97% and 89%, respectively. This result indicated that planting roadside tree was effective for adaptation to urban warming especially in areas of low wind speed.

(b) Health hazard assessment

Fig. 19 shows the cumulative distributions of WBGT within the pedestrian space, which ranged from ground level to a height of 2 m. The cumulative distributions of WBGT showed the same tendency as that of the SET*.

(4) Assessment results

Table 7 summarizes the assessment results in each domain. The presence of roadside trees had positive effects on the mitigation of UHIs and for adaptation to urban warming, but had little effect on mitigation of global warming, under the conditions in this calculation.

5. Conclusions

1) The assessment system proposed by the authors allowed determination of the effects of using greening or highly reflective material on vertical walls from three perspectives of urban warming countermeasure.
2) Green and highly reflective surfaces had a positive impact on the mitigation of global warming and UHIs. However, in terms of adapting to urban warming, greening was not very effective and the highly reflective material had a clearly negative impact under the conditions assumed in this study.
3) Roadside trees had positive impacts on the mitigation of UHIs and the adaptation to urban warming, but had little effect on mitigation of global warming under the conditions assumed in this study.

Acknowledgment

This work was supported by the JSPS Grant-in-Aid for Scientific Research (B) (Grant Number 26289200), and the Grant-in-Aid for JSPS Fellows.

References

Durbin, P. A. (1996). On the k-ε stagnation point anomaly. International Journal of Heat and Fluid Flow 17.

Institute for building environment and energy conservation, 2010: CASBEE-HI manual

Ministry of Environment in Japan, 2013: Study on Heat Island Effects and Countermeasures after the Great East Japan Earthquake

Yumino S., Uchida T., Sasaki K., Kobayashi H., Mochida A., 2015: Total assessment for various environmentally conscious techniques from three perspectives: mitigation of global warming, mitigation of UHIs, and adaptation to urban warming, *Sustainable cities and society* (accepted)

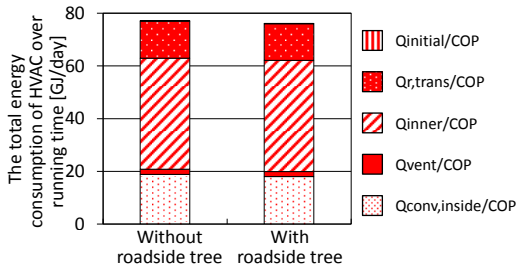

Fig. 16 Energy consumption of the HVAC system

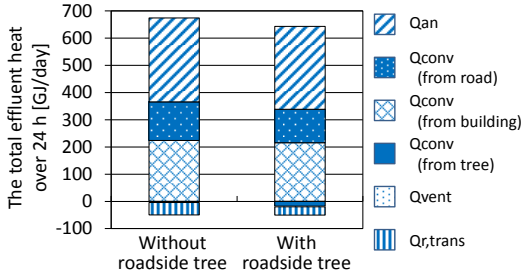

Fig. 17 Net effluent sensible heat from urban surfaces

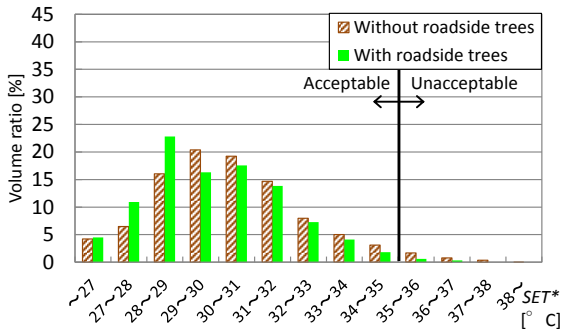

Fig. 18 Cumulative distributions of SET within the pedestrian space*

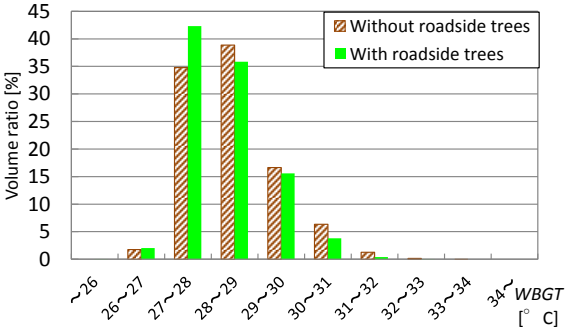

Fig. 19 Cumulative distributions of WBGT within the pedestrian space

Table 7 Assessment result of the effect of roadside trees

Case	Energy consumption of HVAC [GJ/day] [Domain A]	Net effluent sensible heat from urban surfaces [GJ/day] [Domain B]	Acceptable volume ratio evaluated on the basis of SET* (<35°C) [%] [Domain C]		Estimated emergency transport ratio of heatstroke [person/10^6 people/day] [Domain C]	
			Entire pedestrian space	East side	Entire pedestrian space	East side
With roadside tree	77.1	625	97	89	0.42	0.64
Without roadside tree	76.1	592	99	97	0.38	0.55